



Comparisons of polar  
processing  
diagnostics

Z. D. Lawrence et al.

This discussion paper is/has been under review for the journal Atmospheric Chemistry and Physics (ACP). Please refer to the corresponding final paper in ACP if available.

# Comparisons of polar processing diagnostics from 34 years of the ERA-Interim and MERRA reanalyses

Z. D. Lawrence<sup>1</sup>, G. L. Manney<sup>1,2</sup>, K. Minschwaner<sup>1</sup>, M. L. Santee<sup>3</sup>, and A. Lambert<sup>3</sup>

<sup>1</sup>New Mexico Institute of Mining and Technology, Socorro, NM, USA

<sup>2</sup>NorthWest Research Associates, Socorro, NM, USA

<sup>3</sup>Jet Propulsion Laboratory, California Institute of Technology, Pasadena, CA, USA

Received: 24 October 2014 – Accepted: 6 November 2014 – Published: 12 December 2014

Correspondence to: Z. D. Lawrence (zlawrenc@nmt.edu)

Published by Copernicus Publications on behalf of the European Geosciences Union.

Title Page

Abstract

Introduction

Conclusions

References

Tables

Figures



Back

Close

Full Screen / Esc

Printer-friendly Version

Interactive Discussion



## Abstract

We present a comprehensive comparison of polar processing diagnostics derived from the National Aeronautics and Space Administration (NASA) Modern Era Retrospective-analysis for Research and Applications (MERRA) and the European Centre for Medium-Range Weather Forecasts (ECMWF) Interim Reanalysis (ERA-Interim). We use diagnostics that focus on meteorological conditions related to stratospheric chemical ozone loss based on temperatures, polar vortex dynamics, and air parcel trajectories to evaluate the effects these reanalyses might have on polar processing studies. Our results show that the agreement between MERRA and ERA-Interim changes significantly over the 34 years from 1979 through 2013 in both hemispheres, and in many cases improves. By comparing our diagnostics during five time periods when an increasing number of higher quality observations were brought into these reanalyses, we show how changes in the data assimilation systems (DAS) of MERRA and ERA-Interim affected their meteorological data. Many of our stratospheric temperature diagnostics show a convergence toward significantly better agreement, in both hemispheres, after 2001 when Aqua and GOES (Geostationary Operational Environmental Satellite) radiances were introduced into the DAS. Other diagnostics, such as the winter mean volume of air with temperatures below polar stratospheric cloud formation thresholds ( $V_{PSC}$ ) and some diagnostics of polar vortex size and strength, do not show improved agreement between the two reanalyses in recent years when data inputs into the DAS were more comprehensive. The polar processing diagnostics calculated from MERRA and ERA-Interim agree much better than those calculated from earlier reanalysis datasets. We still, however, see fairly large relative biases in many of the diagnostics in years prior to 2002, raising the possibility that the choice of one reanalysis over another could significantly influence the results of polar processing studies. After 2002, we see overall good agreement among the diagnostics, which demonstrates that the ERA-Interim and MERRA reanalyses are equally appropriate choices for polar processing studies of recent Arctic and Antarctic winters.

## Comparisons of polar processing diagnostics

Z. D. Lawrence et al.

Title Page

Abstract

Introduction

Conclusions

References

Tables

Figures



Back

Close

Full Screen / Esc

Printer-friendly Version

Interactive Discussion







## Comparisons of polar processing diagnostics

Z. D. Lawrence et al.

Title Page

Abstract

Introduction

Conclusions

References

Tables

Figures



Back

Close

Full Screen / Esc

Printer-friendly Version

Interactive Discussion



ney et al. (2005b) and Feng et al. (2005) discuss many issues with polar temperatures from the ECMWF 40 year reanalysis (ERA-40), including periods with large spurious vertical oscillations in polar winter temperature profiles (e.g., Simmons et al., 2005). In intercomparisons of temperature diagnostics related to Arctic polar processing of several meteorological analyses, Manney et al. (2003) found that the area with temperatures below PSC thresholds varied by up to 50 % between different analyses, and potential PSC lifetimes differed by several days. Manney et al. (2005a) argued that several reanalyses (the datasets referred to therein as the National Centers for Environmental Prediction and National Center for Atmospheric Research (NCEP-NCAR) reanalysis, NCEP–DOE reanalysis-2, and ERA-40) were unsuitable for stratospheric and polar processing studies.

Since the above-mentioned studies, significant advances have been made in modeling and data assimilation, and several additional datasets have become available for constraining the DAS. Long-term reanalysis systems have become much more widely used, and the long-term records of global meteorology based on observational data that they provide are increasingly critical for climate studies. The growing use of reanalysis datasets demands intercomparisons that quantify the differences between them. While numerous intercomparisons have been done (see, e.g., <https://reanalyses.org/atmosphere/inter-reanalysis-studies-0>), most focus primarily on tropospheric and/or near-surface processes. A few studies have also compared tropical upper tropospheric processes in commonly used reanalyses (e.g., Schoeberl and Dessler, 2011; Fueglistaler et al., 2013). Rieder and Polvani (2013) showed calculations of one polar processing diagnostic,  $V_{\text{PSC}}$ , from three reanalyses. However, no comprehensive intercomparisons of diagnostics pertinent to polar processing in the winter lower stratosphere have been done for the reanalyses that are currently in widespread use. In this paper, we present intercomparisons of polar processing diagnostics derived from the National Aeronautics and Space Administration (NASA) Modern Era Retrospective analysis for Research and Applications (MERRA), and the ECMWF Interim Reanalysis (ERA-Interim). These datasets were chosen for this initial

## Comparisons of polar processing diagnostics

Z. D. Lawrence et al.

Title Page

Abstract

Introduction

Conclusions

References

Tables

Figures



Back

Close

Full Screen / Esc

Printer-friendly Version

Interactive Discussion



study because of their extensive application in numerous stratospheric studies. Rather than focusing on specific seasons and/or a single hemisphere, we present most of our diagnostics for the 1979–2013 record of the reanalyses for both Arctic and Antarctic winters. We examine the potential correlation of biases between the analyses over the  
5 above time period with the timing of changes in observations ingested by their DAS. It is difficult to directly assess the accuracy of reanalyses because there are few, if any, independent measurements (i.e., not used in the assimilation) of temperature available that span the full periods of those analyses; the degree of agreement between re-analyses is thus an important indicator of their inherent uncertainties and the potential  
10 impact of those uncertainties on polar processing studies.

In Sect. 2 we describe the datasets, relevant aspects of the assimilated observations, and the diagnostics and comparison methods we use. The results, presented in Sect. 3, comprise comparisons of polar processing diagnostics based on temperatures, polar vortex dynamics, and trajectory-based temperature histories. Our conclusions are then  
15 summarized and discussed in Sect. 4.

## 2 Data and analysis

### 2.1 NASA Modern Era Retrospective analysis for research and applications

MERRA is a global atmospheric reanalysis that uses version 5.2 of the Goddard Earth Observing System (GEOS) model and assimilation system. It utilizes a combination  
20 of 3D-Var assimilation and Incremental Analysis Update (IAU) (Bloom et al., 1996) to apply corrections from analysis to the forecast model. The MERRA system operates natively on a  $0.5^\circ \times 0.667^\circ$  latitude/longitude grid ( $361 \times 540$  gridpoints) and uses a hybrid sigma-pressure scheme with 72 vertical levels; the vertical resolution in the lower stratosphere is near 1 km. Further details about the MERRA system are given by Rie-  
25 necker et al. (2011). The MERRA data files available from NASA's Global Modeling and Assimilation Office (GMAO) are described by Lucchesi (2012). Except where specified

otherwise, the MERRA temperature data used here are from instantaneous daily files at 12:00 UT on the model levels and grid. However, the potential vorticity (PV) data from MERRA are available only on a reduced  $1^\circ \times 1.25^\circ$  latitude/longitude grid ( $181 \times 288$  gridpoints) with 42 pressure levels; for the purposes of this study, PV is interpolated to match the model levels and grid.

## 2.2 ECMWF Interim reanalysis

ERA-Interim (hereinafter ERA-I) is another global atmospheric data assimilation system. The goal of the ERA-I project was to improve upon ECMWF's previous reanalysis, ERA-40, in advance of their planned next-generation reanalysis. It uses 12 h cycles of 4D-Var assimilation and a T255 spectral model with 60 vertical levels; the vertical resolution in the lower stratosphere is comparable to that of MERRA. The ERA-I system is described in detail by Dee et al. (2011), and the datasets provided by ECMWF from the ERA-I archive are described by Berrisford et al. (2009). In this case, ERA-I data are used on the highest resolution regular latitude/longitude grid publicly available at  $0.75^\circ \times 0.75^\circ$  ( $241 \times 480$  gridpoints) on the 60 model vertical levels; this grid has spacing closest to that of the Gaussian grid associated with the spectral model. As with MERRA, the ERA-I temperature and PV data used in this study are instantaneous at 12:00 UT. However, in this case the PV is derived from the provided relative vorticity, temperature, and pressure fields.

## 2.3 Timelines of assimilated observations

Since satellite observations are the primary constraint on reanalysis products at stratospheric levels, it is useful to consider how the data evolve with the introduction of new missions and instruments: Pawson (2012) noted the effect of the TOVS (Tiros Operational Vertical Sounder) to Advanced TOVS (ATOVS) transition in 1998 on middle and upper stratospheric global temperature anomalies from MERRA and ERA-I. At 5 hPa, he shows that ERA-I temperatures dropped suddenly by about 2 K, while in MERRA

## Comparisons of polar processing diagnostics

Z. D. Lawrence et al.

Title Page

Abstract

Introduction

Conclusions

References

Tables

Figures



Back

Close

Full Screen / Esc

Printer-friendly Version

Interactive Discussion



## Comparisons of polar processing diagnostics

Z. D. Lawrence et al.

Title Page

Abstract

Introduction

Conclusions

References

Tables

Figures



Back

Close

Full Screen / Esc

Printer-friendly Version

Interactive Discussion



the mean annual cycle changed noticeably. Pawson asserts that these distinct discontinuities suggest that more work is needed to properly handle SSU (Stratospheric Sounding Unit) radiances in reanalyses. Fueglistaler et al. (2013) mention that the introduction of COSMIC (Constellation Observing System for Meteorology, Ionosphere, and Climate) GPSRO (Global Positioning Satellite Radio Occultation) temperature data in ERA-I caused a temperature shift in the tropics of about 0.5 K at 100 hPa. Simmons et al. (2014) discuss in detail the various effects of the different satellite missions and instruments on ERA-I temperature data, and perform intercomparisons with MERRA and the Japanese 55 year Reanalysis (JRA55).

In many of our diagnostics, we examine how well MERRA and ERA-I agree over the 1979 to 2013 time period. The observations assimilated in the reanalyses change dramatically over this period, and in some cases there are differences between MERRA and ERA-I in the timing of the changes and the observations included. Figure 1 shows a comparison of the primary satellite datasets assimilated in MERRA and ERA-I, compiled from information in Rienecker et al. (2011), Dee et al. (2011) and Simmons et al. (2014). (See Table 1 for the full names of the instruments and satellites listed in Fig. 1 and throughout this paper.) The colored regions indicate periods of years between which the data input streams change significantly; in other words, marking times when the differences between MERRA and ERA-I might be expected to shift. In this case, we have chosen boundaries at 1987 (when SSM/I was introduced), 1998 (when ATOVS was introduced), 2002 (inclusion of CHAMP in ERA-I, and AIRS and AMSU-A in both reanalyses), and 2007 (when COSMIC was included in ERA-I).

### 2.4 Polar processing diagnostics and intercomparisons

Many of the diagnostics we use are described by Manney et al. (2003, 2005a, 2011), and are designed to assess a wide range of conditions related to polar processing. These diagnostics fall into three categories, focusing on assessment of temperatures, vortex characteristics, or air parcel histories. Taken together, the diagnostics used here provide a comprehensive evaluation of the meteorological conditions pertinent

to chemical processing and ozone destruction in the polar stratosphere. Because our focus is on assessing the effects of reanalysis differences on studies of polar processing that takes place in the lower stratosphere, we focus in this paper on isentropic levels below about 600 K (approximately 25 km, or 30 hPa).

The importance of stratospheric temperatures to the formation of PSCs gives rise to the need for temperature diagnostics. Although some recent studies have suggested that liquid PSCs play a dominant role in activating chlorine (e.g., Wegner et al., 2012; Wohltmann et al., 2013), the formation temperatures of solid nitric acid trihydrate (NAT, Hanson and Mauersberger, 1988) and ice particles remain convenient thresholds for the initiation of chlorine activation processes. In this study, we examine daily minimum temperatures, and calculations of area with temperatures below PSC thresholds (henceforth,  $T_{\min}$  and  $A_{\text{PSC}}$ , respectively). We also use diagnostics derived from  $T_{\min}$  and  $A_{\text{PSC}}$ , such as the number of days during a polar winter with temperatures below PSC thresholds, and the volume of stratospheric air below PSC thresholds ( $V_{\text{PSC}}$ ). For  $A_{\text{PSC}}$ , vertical temperature profiles of the NAT and ice thresholds are derived using climatological profiles of  $\text{HNO}_3$  and  $\text{H}_2\text{O}$  mixing ratios on six per decade pressure levels (Manney et al., 2003), and interpolating to approximately co-located potential temperature surfaces (e.g., the 56.2 and 31.6 hPa levels are referenced to 490 and 580 K, respectively).  $V_{\text{PSC}}$  is calculated by vertically integrating eight potential temperature levels between 390 and 580 K using the altitude approximation introduced by Knox (1998).

Since the polar vortex provides the “containment vessel” within which polar chemical processing takes place (e.g., Schoeberl et al., 1992), we also compare diagnostics that characterize vortex strength and size. These include daily maximum PV gradients (one measure of vortex strength, e.g., Manney et al., 2011, and references therein), and the area of a hemisphere covered by the vortex (henceforth, MPVG and  $A_{\text{vort}}$ , respectively). In addition to the total area of the vortex, we also calculate the area of the vortex that receives sunlight each day, since the photochemical processes involved in chlorine catalyzed ozone depletion require sunlight (e.g., Solomon, 1999). Finally, we

## Comparisons of polar processing diagnostics

Z. D. Lawrence et al.

[Title Page](#)[Abstract](#)[Introduction](#)[Conclusions](#)[References](#)[Tables](#)[Figures](#)[Back](#)[Close](#)[Full Screen / Esc](#)[Printer-friendly Version](#)[Interactive Discussion](#)

## Comparisons of polar processing diagnostics

Z. D. Lawrence et al.

Title Page

Abstract

Introduction

Conclusions

References

Tables

Figures

◀

▶

◀

▶

Back

Close

Full Screen / Esc

Printer-friendly Version

Interactive Discussion



vertically integrate  $A_{\text{vort}}$  in the same manner as  $A_{\text{PSC}}$  to derive the vortex fraction of low temperature air (i.e.,  $V_{\text{PSC}}/V_{\text{vort}}$ ). In all cases we use isentropic surfaces, and scale PV into “vorticity units” ( $\text{s}^{-1}$ ) (Dunkerton and Delisi, 1986; Manney et al., 1994b). MPVG is calculated as described by Manney et al. (1994a): scaled PV (sPV) is numerically differentiated with respect to equivalent latitude (i.e., the value of the latitude circle enclosing the same area as a given PV contour); if the maximum gradient occurs at an equivalent latitude poleward of  $\pm 80^\circ$ , we consider the vortex to be undefined and set the maximum gradient equal to zero. To calculate the area of the polar vortex, we use the  $1.4 \times 10^{-4} \text{ s}^{-1}$  sPV contour as a simple proxy for the vortex edge (e.g., Manney et al., 2007). The total area of the vortex is then the area of the contour. The sunlit area is the area inside the vortex-edge contour that is equatorward of the daily polar night latitude at 12:00 UT.

One of our diagnostics is best described as a hybrid temperature-vortex diagnostic. It is the concentricity of the polar vortex with regions of temperatures below the NAT PSC threshold (henceforth referred to as vortex-temperature concentricity, or VTC). VTC is adapted from the concept of concentricity as discussed by Mann et al. (2002). We calculate it using the simple formula

$$\text{VTC} = 1 - \frac{\text{GCDist}(\text{Vortex Centroid, Cold Region Centroid})}{\text{GCDist}(\text{Pole, Equiv. Lat. of Vortex Edge})} \quad (1)$$

where  $\text{GCDist}(x, y)$  is the great circle distance between  $x$  and  $y$ . This definition provides an intuitive picture of the vortex/temperature relationships under extreme conditions: a maximum value of 1 for collocated centroids (completely concentric), and values less than or equal to 0 for a cold region centroid approximately at or outside the vortex edge. Centroid locations are calculated as described by Mitchell et al. (2011) and Seviour et al. (2013), with the  $1.4 \times 10^{-4} \text{ s}^{-1}$  sPV and pressure-dependent NAT PSC temperatures as the edge values for the vortex and cold regions, respectively. For simplicity, we only calculated one centroid for each field. This means that, for example, during vortex-split sudden stratospheric warming (SSW) events, offspring vortices



## Comparisons of polar processing diagnostics

Z. D. Lawrence et al.

Title Page

Abstract

Introduction

Conclusions

References

Tables

Figures



Back

Close

Full Screen / Esc

Printer-friendly Version

Interactive Discussion



SSW (Coy and Pawson, 2014). The departure of the daily average differences (thick black line) from zero suggests a persistent relative bias between the two reanalyses that dominates for much of the 34 years. Since this bias varies over the season, we define monthly relative biases between the datasets as the monthly averaged mean daily differences over the years in each of the periods defined in Fig. 1. These quantities provide a compact means of summarizing the agreement between the datasets for a given month and subset of years, and of comparing the magnitude of differences between comparison periods for a particular diagnostic. We refer to these as “relative” biases to emphasize that they represent biases between the two datasets, as opposed to an assessment of absolute accuracy of either. For the rest of this paper, we use the convention of subtracting ERA-I from MERRA (that is, MERRA minus ERA-I) to calculate monthly relative biases. As such, differences in a diagnostic greater (less) than zero indicate that, on average, MERRA is greater (less) than ERA-I.

### 3.2 Temperature diagnostic intercomparisons

The seasonal progression of polar minimum temperatures provides an indication of when conditions favor the development of PSCs. The dependence of PSC formation on a temperature threshold implies that conclusions drawn from the  $T_{\min}$  diagnostic are most sensitive to differences at the beginning and ends of the season when minimum temperatures first drop below or rise above PSC thresholds. For the Arctic, these periods are typically around the beginning of December and mid-March, respectively, but large interannual variability and the common occurrence of mid-winter SSWs can result in much earlier or later threshold dates in individual years (Manney et al., 2005a, and references therein). In the Antarctic, the threshold periods tend to be in the first half of May and in mid-October. Figure 3 shows the monthly relative biases between MERRA and ERA-I at the 580 K level ( $\sim 30$  hPa, corresponding to an approximate  $T_{\text{NAT}}$  of 193 K). For years preceding 2002, MERRA consistently has lower minimum temperatures than ERA-I. The Antarctic relative biases in this period are particularly large, with differences between  $-5$  to  $-6$  K in some months, in contrast to the largest differences

## Comparisons of polar processing diagnostics

Z. D. Lawrence et al.

Title Page

Abstract

Introduction

Conclusions

References

Tables

Figures



Back

Close

Full Screen / Esc

Printer-friendly Version

Interactive Discussion



in the Arctic, which are about  $-1.4$  K. Differences in 1998–2001, after the introduction of the ATOVS instruments, but before the introduction of the Aqua instruments, are significantly reduced over those prior to 1998. In both hemispheres, there is a distinct shift in agreement after the introduction of the Aqua instruments from 2002 onward (likely due to the vast increase in the number of observations included by assimilating AIRS data). This is especially easy to see for the Antarctic, where the relative biases are reduced to values akin to those in the Arctic. In the Northern Hemisphere (NH), the shift marks the first period in which ERA-I minimum temperatures become consistently lower than those from MERRA. At lower levels down to about 460 K (not shown), the  $T_{\min}$  relative biases are smaller in magnitude (e.g., at 490 K they are between  $-0.4$  and  $0.7$  K in the Arctic, and  $-2$  to  $2$  K in the Antarctic), and have different seasonal variations, with ERA-I having comparatively more months in the first three time periods with lower minimum temperatures.

To examine the global variation of temperature differences between MERRA and ERA-I, Fig. 4 shows maps of mean temperature differences (averaged over the time periods of interest from Fig. 1) for the months with the largest relative  $T_{\min}$  biases in Fig. 3. The maps for the Arctic, with the more symmetric color bar, clearly demonstrate that the regions where MERRA is colder tend to be mostly confined between  $\pm 90^\circ$  longitude and poleward of  $60^\circ$  latitude. This is a preferred direction for the polar vortex and cold region to be shifted off the pole in Arctic winters (e.g., Waugh and Randel, 1999). Outside of this area, ERA-I temperatures are, for the most part, lower than those from MERRA. In the Southern Hemisphere (SH), the first three time periods show that the regions that are colder in MERRA are fairly symmetric poleward of the  $60^\circ$  S latitude circle. Examination of the mean temperature fields (not shown) for these periods suggests that larger biases are associated with lower temperatures. The maps for the following two time periods, from 2002 to 2013, demonstrate that the change seen in Fig. 3 reflects a distinct shift throughout the polar regions: the largest temperature differences during these periods are confined to relatively small regions, and overall the temperature differences lie between  $\pm 0.4$  K in both hemispheres. Simmons et al. (2014)

show extratropical zonal-mean temperature differences between ERA-I and MERRA at 30 hPa that indicate the extratropics ( $\pm 20\text{--}90^\circ$  latitude) are colder in ERA-I than in MERRA for most of the reanalysis period. The results shown here are generally consistent with that finding, but suggest that this result does not hold true poleward of  $\pm 60^\circ$  latitude in winter/spring.

The number of days below PSC thresholds, a diagnostic derived from  $T_{\min}$ , for winters in the 1979 through 2013 period is shown at 490 K ( $\sim 56$  hPa) for both hemispheres in Fig. 5; we show days below  $T_{\text{ice}}$ , rather than  $T_{\text{NAT}}$ , in the Antarctic because the period with temperatures below either threshold is much longer, making the differences clearer for the lower ice threshold. This diagnostic indicates the approximate duration of the period with conditions conducive to polar processing. Overall, the number of cold days from ERA-I is greater than the number from MERRA in both hemispheres. The Antarctic differences before 2002 are quite large, with some years showing ERA-I having over 10 more days with temperatures below the ice PSC threshold than MERRA. At levels up to 580 K (not shown), the situation in the Antarctic is opposite; that is, there are significantly more days with temperatures below the ice PSC threshold in MERRA than in ERA-I. These results, along with those discussed about  $T_{\min}$ , suggest that not only may the choice of dataset have a large influence on analysis and modeling of polar processes in the Antarctic for years preceding 2002, but also that effects may vary qualitatively and quantitatively in the vertical. In contrast to the Antarctic, the magnitude of differences in the Arctic at higher levels up to 580 K are largely similar to those at 490 K, but with MERRA having more cold days than ERA-I.

Average values for the total area with temperatures below the NAT threshold at 580 K are displayed in Fig. 6. The Arctic maximum mean area is just above 3% of the hemisphere for ERA-I, while MERRA reaches nearly 4%. In a similar fashion, the Antarctic maximum mean area is about 11% of the hemisphere for ERA-I, while that for MERRA reaches nearly 12%. Differences in these mean values between the reanalyses vary considerably with the season in both hemispheres. Figure 7 shows the corresponding monthly relative biases for  $A_{\text{NAT}}$ . Here it is worth noting that the low biases in the last

## Comparisons of polar processing diagnostics

Z. D. Lawrence et al.

Title Page

Abstract

Introduction

Conclusions

References

Tables

Figures



Back

Close

Full Screen / Esc

Printer-friendly Version

Interactive Discussion



## Comparisons of polar processing diagnostics

Z. D. Lawrence et al.

Title Page

Abstract

Introduction

Conclusions

References

Tables

Figures



Back

Close

Full Screen / Esc

Printer-friendly Version

Interactive Discussion



month of the season in each hemisphere are expected as these include many days that have zero biases because minimum temperatures have risen above the NAT threshold in both reanalyses. Consistent with the  $T_{\min}$  relative biases, there is much closer agreement after the first three periods. The relatively frequent occurrence of warm Arctic winters after 1998 (e.g., Manney et al., 2005a) suggests that the third Northern Hemisphere period might be less easily compared with the previous period with unusually cold Arctic winters (e.g., Pawson and Naujokat, 1999), but the marked decreases of relative biases in the SH still indicate a substantial effect due to changes in assimilated observations. In most cases the relative biases are positive, indicating that MERRA tends to have larger cold regions than ERA-I at this level in both hemispheres. For levels below 580 K, down into the upper troposphere/lower stratosphere (UTLS) region at 390 K (not shown), MERRA still tends to have larger cold regions than ERA-I, but the conditions are different: the relative biases are much smaller in all periods, generally lying between  $-1$  and  $1$  % in the Antarctic, and  $-0.4$  and  $0.4$  % in the Arctic. Although the relative biases are smaller, the same convergence towards better agreement we see at 580 K is not always seen at levels below 520 K, especially in the Arctic.

### 3.3 Vortex diagnostic intercomparisons

Maximum PV gradients (MPVG) indicate the strength of the polar vortex as a barrier to transport and mixing of air from lower latitudes and the cold vortex air where chlorine activation takes place (e.g., Manney et al., 2011). The seasonal evolution and mean values of maximum PV gradients at 490 K are shown in Fig. 8. The primary difference between the hemispheres is seen in the average values; the Arctic maximum gradients tend to level off at around  $10^{-5} \text{ s}^{-1} \text{ deg}^{-1}$  early in the season, while the Antarctic maximum gradients steadily increase up to approximately  $1.7 \times 10^{-5} \text{ s}^{-1} \text{ deg}^{-1}$  near the end of the season. The MPVG relative biases are shown in Fig. 9. Note that the scaling of the values is  $10^{-6} \text{ s}^{-1} \text{ deg}^{-1}$ . This means a relative bias of 1 would be 1/5 the height of a grid-box from Fig. 8. As such, the relative biases are overall quite small, but the monthly and comparison period variations still provide useful information. For instance,

the greater MERRA MPVGs in the months when the vortex usually weakens (March or April in the Arctic, November in the Antarctic) suggest that the polar vortices as represented by ERA-I tend to weaken earlier than those in MERRA. Furthermore, a shift in agreement contemporaneous with those seen in Figs. 3 and 7 is also present. In this case, however, the relative biases increase considerably for the Northern Hemisphere rather than decrease. This behavior, with agreement in the SH (NH) improving (degrading) slightly, is also seen at other vertical levels between 460 and 580 K.

Similar to  $A_{PSC}$ , the sunlit area of the vortex provides an approximate quantitative measure of the area on a given vertical level where chlorine-catalyzed ozone destruction can take place. Different sunlit area diagnostics have been used in detailed polar processing studies to establish correlations between the coverage (e.g., Feng et al., 2007) and duration (e.g., Rex et al., 1999; Livesey et al., 2014, in preparation) of sunlight and ozone loss; these diagnostics are usually somewhat computationally intensive, whereas the diagnostic used here (described in Sect. 2.4 above) is simple enough to compute for multiple long-term datasets. Figure 10 shows time series averages and ranges of the sunlit vortex diagnostic as a fraction of a hemisphere at 490 K. The seasonal variations of the sunlit vortex are very similar in both datasets. There are, however, small biases that can be seen: the ERA-I Arctic polar vortex tends to be filled with slightly more sunlight than the MERRA vortex, while in the Antarctic, the bias changes over the season. Consistent with this, the sunlit vortex monthly relative biases in Fig. 11 show predominantly negative values in the Arctic (indicating the bias towards ERA-I), and biases that change sign in the Antarctic. Like the NH MPVG relative biases, the NH sunlit vortex relative biases increase to a maximum by the 5th time period (2007–2013) of Fig. 1. The overall maximum relative biases occur in November and February of this final time period, both months when a substantial portion of the vortex is typically in darkness, and when varying sunlight may affect chlorine activation whenever temperatures are low enough for PSC formation. In contrast to the NH, the SH relative biases improve slightly over the reanalysis period. Biases of the small magnitude shown here are unlikely to have large effects on polar processing in either hemisphere,

## Comparisons of polar processing diagnostics

Z. D. Lawrence et al.

[Title Page](#)[Abstract](#)[Introduction](#)[Conclusions](#)[References](#)[Tables](#)[Figures](#)[Back](#)[Close](#)[Full Screen / Esc](#)[Printer-friendly Version](#)[Interactive Discussion](#)



## Comparisons of polar processing diagnostics

Z. D. Lawrence et al.

Title Page

Abstract

Introduction

Conclusions

References

Tables

Figures



Back

Close

Full Screen / Esc

Printer-friendly Version

Interactive Discussion



Exceptions to this are in 2007–2013 in the NH, when slightly smaller MERRA  $V_{\text{vort}}$  values emphasize the  $\sim 0.01$  larger  $V_{\text{PSC}}/V_{\text{vort}}$  values seen in MERRA, and in 1979–1987 in the SH, when the  $\sim 0.02$  larger ERA-I  $V_{\text{PSC}}/V_{\text{vort}}$  values represent larger cold fractions of smaller vortices. This analysis demonstrates several caveats for comparisons of diagnostics that rely on vertical integration, time averages, or combinations of both. Their dependence on time and/or altitude can lead to cancellations and smoothing when integrated and/or time-averaged, making comparisons of the final results difficult to interpret since agreement (or lack thereof) can come about for the wrong reasons. In this case, the agreement of winter mean  $V_{\text{PSC}}$ ,  $V_{\text{vort}}$ , and  $V_{\text{PSC}}/V_{\text{vort}}$  between the re-analyses was affected by the representation of several conditions. Because the relative biases in  $A_{\text{PSC}}$  and  $A_{\text{vort}}$  change differently with time and altitude, better agreement at some levels does not necessarily correlate with better confidence in our knowledge of  $V_{\text{PSC}}$ , and consequently  $V_{\text{PSC}}/V_{\text{vort}}$ . This suggests that these diagnostics function better as qualitative measures, and argues for considerable caution in interpretation of their time variations or trends.

The concentricity of the vortex with regions of air with  $T \leq T_{\text{NAT}}$  (VTC) has not been widely used in polar processing studies. However, Mann et al. (2002), using a concentricity diagnostic different from that defined here, found that different values led to dramatically different patterns of denitrification in model simulations of NAT particle growth and evaporation because differences in the position of the cold region relative to the strong winds bounding the vortex can result in large differences in the amount of time air spends in cold regions of comparable size (Manney et al., 2003). Using idealized model simulations with a constant vortex field and cold regions ranging from highly concentric to nonconcentric, Mann et al. showed that concentricity affected denitrification independent of any variations in the vortex itself. Since the concentricity calculation requires both the vortex and a cold region to be defined, intercomparisons of the resulting discontinuous time series can be difficult to interpret. Therefore, we present this diagnostic as occurrence frequencies of the range of VTC values, normalized by the total number of days on which VTC was calculated for each reanalysis. Figure 14 shows

## Comparisons of polar processing diagnostics

Z. D. Lawrence et al.

Title Page

Abstract

Introduction

Conclusions

References

Tables

Figures



Back

Close

Full Screen / Esc

Printer-friendly Version

Interactive Discussion



the results at the 490 K level. The total number of days shown corresponds to the number of days with a valid VTC value summed over the years from the comparison time periods defined in Fig. 1 and used in the monthly relative bias plots. As evidenced by the non-overlapping colors, in most cases the ERA-I vortices spend more time at higher concentricity values (within the 0.8 to 1.0 range) in both hemispheres. Consistent with the number of days below PSC thresholds shown in Fig. 5, ERA-I also tends to have more valid VTC days than MERRA in both hemispheres. The detailed implications of differences in concentricity are difficult to assess, but the results of Mann et al. (2002) and Manney et al. (2003) suggest that greater concentricity in ERA-I could bias model runs driven by that reanalysis towards longer-lasting PSCs, greater denitrification, and enhanced chlorine activation.

### 3.4 Trajectory diagnostic intercomparisons

Temperature histories along air parcel trajectories provide further information about polar processing potential beyond what can be obtained from the simple diagnostics described above. For these intercomparisons, we use isentropic trajectory calculations on the 490 K surface. As discussed by Manney et al. (2003), although neglecting cross-isentropic motion would not be suitable for detailed polar processing studies, this simplification allows us to efficiently run and analyze a large number of parcels for extensive intercomparisons. Following Manney et al. (2003, 2005a), we consider only the parcels that are initialized in regions with temperatures less than 195 K. With this initial filter, we examine the total and continuous amounts of time that these parcels spend at temperatures below 195 K (TT195 and CT195, respectively) before and after the initialization date, and the mean temperature of the parcels over the full run. The TT195 diagnostic captures the total exposure of an air mass to temperatures low enough for PSC formation and thus acts as a proxy for cumulative chlorine activation; CT195 better represents the potential lifetime of a PSC and is thus more directly relevant for denitrification, since sufficiently long continuous time at low temperatures allows PSC particles to grow to sizes large enough for sedimentation to occur (Manney et al., 2003, 2005a). Here we



## Comparisons of polar processing diagnostics

Z. D. Lawrence et al.

Title Page

Abstract

Introduction

Conclusions

References

Tables

Figures



Back

Close

Full Screen / Esc

Printer-friendly Version

Interactive Discussion



even for early years, thus lending confidence in transport calculations using winds from these two reanalyses. The same cannot be said for early years in the SH, where many fewer observations were available in the 1980s and 1990s, allowing differences in the models and DAS to dominate the data constraints. This resulted in systematic differences in temperature histories that are consistent with the large relative biases seen in direct temperature diagnostics (e.g., Figs. 3 through 7). Overall, the agreement of the trajectory diagnostics from MERRA and ERA-I is much better than that from older analyses: in previous intercomparison studies, Manney et al. (2003, 2005a) found very large differences in trajectory runs driven by fields from earlier analyses/reanalyses. Discrepancies in 465 K trajectories for average TT195 were as large in magnitude as 5 days for the NH and 7 days for SH, with discrepancies in average CT195 in both hemispheres up to 2.5 days. For 10 January 1996 (shown here in Fig. 15), the time series of average parcel histories calculated by Manney et al. (2003) showed differences as large as 10 K on some days; in addition, the five analyses compared in that study showed qualitatively very different distributions of TT195 and CT195. Large qualitative differences were also seen between the different analyses in September 2002 (Manney et al., 2005a), in contrast to the small biases and good qualitative agreement seen here in Fig. 16 (middle panels). The improvements in the agreement between MERRA and ERA-I over that between earlier analyses, which largely ingested the same data, demonstrate the degree of improvement in the models and DAS techniques over the past decade.

## 4 Discussion and conclusions

We have presented comparisons of stratospheric polar processing diagnostics derived from the MERRA and ERA-Interim reanalyses for Arctic and Antarctic winters from 1979 through 2013. By using temperature, vortex, and trajectory diagnostics, we have comprehensively explored the major aspects of the dynamical fields that chemical destruction of polar ozone in the lower stratosphere is sensitive to. In addition, we have

characterized how agreement between the two reanalyses evolved over the 1979–2013 period as assimilated observations changed. To do this, we compared the temperature and vortex diagnostics during five time periods bounded by large changes in the datasets that were assimilated. Most of the comparisons are shown using calculations of monthly relative biases, which are monthly means of the daily average differences between MERRA and ERA-I. Our primary conclusions are as follows:

- Comparisons of temperature diagnostics derived from MERRA and ERA-I show a major shift towards better agreement around 2002, especially at levels above about 490 K. At 580 K (around 30 hPa), ERA-I tends to have more days with lower temperatures, whereas MERRA tends to have larger regions of cold air. These results are consistent between the hemispheres.
- The comparisons of winter mean  $V_{PSC}$  have a complex dependence on time and altitude as evidenced by the  $A_{NAT}$  relative biases. The shift towards better agreement in both hemispheres for  $A_{NAT}$  above 490 K was not enough to make the comparisons of winter mean  $V_{PSC}$  agree better.
- Comparisons based on differences of winter mean  $V_{PSC}/V_{vort}$  can be complicated because of the dependence on  $V_{PSC}$  and  $V_{vort}$  individually. Since MERRA tends to have larger regions of cold air (larger  $V_{PSC}$ ) than ERA-I, and similarly or smaller-sized vortices in recent periods, MERRA also has larger vortex fractions of cold air in years beyond  $\sim 1992$ .
- The vortex diagnostic comparisons are more complicated than those of the temperature diagnostics. In many cases the relative biases do not improve; some even increase over the 1979–2013 time period, especially in the Arctic. These biases, however, tend to be small.
- Isentropic trajectory runs driven by MERRA and ERA-I give very similar results overall. We found that in the Northern Hemisphere, the trajectory diagnostics

## Comparisons of polar processing diagnostics

Z. D. Lawrence et al.

[Title Page](#)[Abstract](#)[Introduction](#)[Conclusions](#)[References](#)[Tables](#)[Figures](#)[Back](#)[Close](#)[Full Screen / Esc](#)[Printer-friendly Version](#)[Interactive Discussion](#)



assimilated datasets can still be important factors even when the temperature fields are quite well constrained by data.

The results in this paper provide strong evidence that the agreement between MERRA and ERA-I evolves with their changing data inputs. While this is an unsurprising result, it confirms that changes in the assimilated observations often directly influence the analyzed temperature fields more than the model and assimilation characteristics do. Only when observations were sparse and nearly identical in MERRA and ERA-I (such as in the SH before 2002) did we see large differences that indicated the effect of model and assimilation system differences. Our results further indicate that ERA-I's assimilation of measurements from GPSRO and other additional instruments that are not used in MERRA in the final observation period (2007 through 2013) results in only a small improvement in stratospheric temperature diagnostics that already show good agreement after 2002. The most recent period has the best agreement for most of the diagnostics shown. This has been noted elsewhere: Martineau and Son (2010) found that MERRA and ERA-I had the lowest biases among other reanalyses in comparison to COSMIC temperatures during the 2009 Arctic sudden stratospheric warming.

Further work is planned to more fully characterize the agreement of diagnostics of polar processing between recent reanalyses, and the importance of these diagnostics to polar processing studies. In the context of the SPARC (Stratosphere–troposphere Processes And their Role in Climate) Reanalysis Intercomparison Project (S-RIP), we plan to extend these intercomparisons to include the NCEP Climate Forecast System Reanalysis (NCEP/CFSR, Saha et al., 2010) and the Japanese 55 year Reanalysis (JRA55, Ebita et al., 2011). In addition, two of the diagnostics introduced (sunlit vortex area and VTC) have not been widely used in previous polar processing studies. Work in progress applying sunlit vortex area and VTC to disturbed vs. more quiescent Arctic winters will help establish the sensitivity of polar processing and ozone loss to the conditions characterized by these diagnostics.

## Comparisons of polar processing diagnostics

Z. D. Lawrence et al.

Title Page

Abstract

Introduction

Conclusions

References

Tables

Figures



Back

Close

Full Screen / Esc

Printer-friendly Version

Interactive Discussion



*Acknowledgements.* The authors would like to thank the personnel responsible for producing the ERA-Interim and MERRA reanalysis datasets. ERA-Interim data was made available by ECMWF, Shinfield Park, Reading, UK; MERRA data was provided by the GMAO, Greenbelt, Maryland, USA. Thanks to David Tan and Steven Pawson for helpful comments and suggestions regarding this work, Nathaniel Livesey for help with setting up the trajectory code, and Brian Knosp, William Daffer, and the JPL Microwave Limb Sounder team for computing and data management support. Work at the Jet Propulsion Laboratory, California Institute of Technology, was done under contract with the National Aeronautics and Space Administration.

## References

- 10 Berrisford, P., Dee, D. P., Fielding, K., Fuentes, M., Kallberg, P., Kobayashi, S., and Uppala, S.: The ERA-Interim Archive, ERA report series, Shinfield Park, Reading, European Centre for Medium-Range Weather Forecasts, 1–16, 2009. 31367
- Bloom, S. C., Takacs, L. L., da Silva, A. M., and Ledvina, D.: Data assimilation using incremental analysis updates, *Mon. Weather Rev.*, 124, 1256–1271, 1996. 31366
- 15 Brakebusch, M., Randall, C. E., Kinnison, D. E., Tilmes, S., Santee, M. L., and Manney, G. L.: Evaluation of whole atmosphere community climate model simulations of ozone during Arctic winter 2004–2005, *J. Geophys. Res.*, 118, 2673–2688, 2013. 31364
- Charlton-Perez, A. J., Hawkins, E., Eyring, V., Cionni, I., Bodeker, G. E., Kinnison, D. E., Akiyoshi, H., Frith, S. M., Garcia, R., Gettelman, A., Lamarque, J. F., Nakamura, T., Pawson, S., Yamashita, Y., Bekki, S., Braesicke, P., Chipperfield, M. P., Dhomse, S., Marchand, M., Mancini, E., Morgenstern, O., Pitari, G., Plummer, D., Pyle, J. A., Rozanov, E., Scinocca, J., Shibata, K., Shepherd, T. G., Tian, W., and Waugh, D. W.: The potential to narrow uncertainty in projections of stratospheric ozone over the 21st century, *Atmos. Chem. Phys.*, 10, 9473–9486, doi:10.5194/acp-10-9473-2010, 2010. 31364
- 20 Coy, L. and Pawson, S.: The major stratospheric sudden warming of January 2013: analyses and forecasts in the GEOS-5 data assimilation system, *Mon. Weather Rev.*, doi:10.1175/MWR-D-14-00023.1, in press, 2014. 31372
- Davies, S., Chipperfield, M. P., Carslaw, K. S., Sinnhuber, B.-M., Anderson, J. G., Stimpfle, R. M., Wilmouth, D. M., Fahey, D. W., Popp, P. J., Richard, E. C., von der Gathen, P.,

## Comparisons of polar processing diagnostics

Z. D. Lawrence et al.

Title Page

Abstract

Introduction

Conclusions

References

Tables

Figures



Back

Close

Full Screen / Esc

Printer-friendly Version

Interactive Discussion



Jost, H., and Webster, C. R.: Modeling the effect of denitrification on Arctic ozone depletion during winter 1999/2000, *J. Geophys. Res.*, 107, SOL 65-1–SOL 65-18, 2002. 31364

Dee, D. P., Uppala, S. M., Simmons, A. J., Berrisford, P., Poli, P., Kobayashi, S., Andrae, U., Balmaseda, M. A., Balsamo, G., Bauer, P., Bechtold, P., Beljaars, A. C. M., van de Berg, L., Bidlot, J., Bormann, N., Delsol, C., Dragani, R., Fuentes, M., Geer, A. J., Haimberger, L., Healy, S. B., Hersbach, H., Hólm, E. V., Isaksen, I., Kållberg, P., Köhler, M., Matricardi, M., McNally, A. P., Monge-Sanz, B. M., Morcrette, J.-J., Park, B.-K., Peubey, C., de Rosnay, P., Tavolato, C., Thépaut, J.-N., and Vitart, F.: The ERA-Interim reanalysis: configuration and performance of the data assimilation system, *Q. J. Roy. Meteor. Soc.*, 137, 553–597, 2011. 31367, 31368

Dunkerton, T. J. and Delisi, D. P.: Evolution of potential vorticity in the winter stratosphere of January-February 1979, *J. Geophys. Res.*, 91, 1199–1208, 1986. 31370

Ebita, A., Kobayashi, S., Ota, Y., Moriya, M., Kumabe, R., Onogi, K., Harada, Y., Yasui, S., Miyaoka, K., Takahashi, K., Kamahori, H., Kobayashi, C., Endo, H., Soma, M., Oikawa, Y., and Ishimizu, T.: The Japanese 55-year Reanalysis “JRA-55”: an interim report, *SOLA*, 7, 149–152, 2011. 31384

Feng, W., Chipperfield, M. P., Roscoe, H. K., Remedios, J. J., Waterfall, A. M., Stiller, G. P., Glatthor, N., Höpfner, M., and Wang, D.-Y.: Three-dimensional model study of the Antarctic ozone hole in 2002 and comparison with 2000, *J. Atmos. Sci.*, 62, 822–837, 2005. 31365

Feng, W., Chipperfield, M. P., Davies, S., von der Gathen, P., Kyrö, E., Volk, C. M., Ulanovsky, A., and Belyaev, G.: Large chemical ozone loss in 2004/2005 Arctic winter/spring, *Geophys. Res. Lett.*, 34, L09803, doi:10.1029/2006GL029098, 2007. 31376

Fueglistaler, S., Liu, Y. S., Flannaghan, T. J., Haynes, P. H., Dee, D. P., Read, W. J., Remsberg, E. E., Thomason, L. W., Hurst, D. F., Lanzante, J. R., and Bernath, P. F.: The relation between atmospheric humidity and temperature trends for stratospheric water, *J. Geophys. Res.*, 118, 1052–1074, 2013. 31365, 31368

Hanson, D. and Mauersberger, K.: Laboratory studies of the nitric acid trihydrate: implications for the south polar stratosphere, *Geophys. Res. Lett.*, 15, 855–858, 1988. 31369

Harris, N. R. P., Lehmann, R., Rex, M., and von der Gathen, P.: A closer look at Arctic ozone loss and polar stratospheric clouds, *Atmos. Chem. Phys.*, 10, 8499–8510, doi:10.5194/acp-10-8499-2010, 2010. 31364

## Comparisons of polar processing diagnostics

Z. D. Lawrence et al.

Title Page

Abstract

Introduction

Conclusions

References

Tables

Figures



Back

Close

Full Screen / Esc

Printer-friendly Version

Interactive Discussion



Hitchcock, P., Shepherd, T. G., and McLandress, C.: Past and future conditions for polar stratospheric cloud formation simulated by the Canadian Middle Atmosphere Model, *Atmos. Chem. Phys.*, 9, 483–495, doi:10.5194/acp-9-483-2009, 2009. 31364

Knox, J. A.: On converting potential temperature to altitude in the middle atmosphere, *Eos Trans. AGU*, 79, 376–378, 1998. 31369

Livesey, N. J.: Aura Microwave Limb Sounder Lagrangian Trajectory Diagnostics Users' guide and file description document, Tech. Rep., JPL, available at: [http://mls.jpl.nasa.gov/data/ltl\\_d.php](http://mls.jpl.nasa.gov/data/ltl_d.php) (last access: 20 October 2014), 2013. 31371

Livesey, N. J., Santee, M. L., Manney, G. L., and Rex, M.: Polar stratospheric ozone loss quantification: a Match approach applied to Aura Microwave Limb Sounder observations, to be submitted to *Atmos. Chem. Phys. Discuss.*, 2014. 31376

Lucchesi, R., 2012: File Specification for MERRA Products. GMAO Office Note No. 1 (Version 2.3), Greenbelt, Maryland, National Aeronautics and Space Administration Global Modeling and Assimilation Office, 82 pp., available from [http://gmao.gsfc.nasa.gov/pubs/office\\_notes](http://gmao.gsfc.nasa.gov/pubs/office_notes), 2012. 31366

Mann, G. W., Davies, S., Carslaw, K. S., Chipperfield, M. P., and Kettleborough, J.: Polar vortex concentricity as a controlling factor in Arctic denitrification, *J. Geophys. Res.*, 107, 4663, doi:10.1029/2002JD002102, 2002. 31370, 31378, 31379

Manney, G. L., Zurek, R. W., Gelman, M. E., Miller, A. J., and Nagatani, R.: The anomalous Arctic lower stratospheric polar vortex of 1992–1993, *Geophys. Res. Lett.*, 21, 2405–2408, 1994a. 31363, 31370

Manney, G. L., Zurek, R. W., O'Neill, A., and Swinbank, R.: On the motion of air through the stratospheric polar vortex, *J. Atmos. Sci.*, 51, 2973–2994, 1994b. 31370

Manney, G. L., Sabutis, J. L., Pawson, S., Santee, M. L., Naujokat, B., Swinbank, R., Gelman, M. E., and Ebisuzaki, W.: Lower stratospheric temperature differences between meteorological analyses in two cold Arctic winters and their impact on polar processing studies, *J. Geophys. Res.*, 108, 8328, doi:10.1029/2001JD001149, 2003. 31365, 31368, 31369, 31371, 31378, 31379, 31381

Manney, G. L., Allen, D. R., Krüger, K., Naujokat, B., Santee, M. L., Sabutis, J. L., Pawson, S., Swinbank, R., Randall, C. E., Simmons, A. J., and Long, C.: Diagnostic comparison of meteorological analyses during the 2002 Antarctic winter, *Mon. Weather Rev.*, 133, 1261–1278, 2005a. 31365, 31368, 31371, 31372, 31375, 31379, 31381

**Comparisons of polar processing diagnostics**

Z. D. Lawrence et al.

[Title Page](#)[Abstract](#)[Introduction](#)[Conclusions](#)[References](#)[Tables](#)[Figures](#)[Back](#)[Close](#)[Full Screen / Esc](#)[Printer-friendly Version](#)[Interactive Discussion](#)

Manney, G. L., Krüger, K., Sabutis, J. L., Sena, S. A., and Pawson, S.: The remarkable 2003–2004 winter and other recent warm winters in the Arctic stratosphere since the late 1990s, *J. Geophys. Res.*, 110, D04107, doi:10.1029/2004JD005367, 2005b. 31364

Manney, G. L., Daffer, W. H., Zawodny, J. M., Bernath, P. F., Hoppel, K. W., Walker, K. A., Knosp, B. W., Boone, C., Remsberg, E. E., Santee, M. L., Harvey, V. L., Pawson, S., Jackson, D. R., Deaver, L., McElroy, C. T., McLinden, C. A., Drummond, J. R., Pumphrey, H. C., Lambert, A., Schwartz, M. J., Froidevaux, L., McLeod, S., Takacs, L. L., Suarez, M. J., Trepte, C. R., Cuddy, D. C., Livesey, N. J., Harwood, R. S., and Waters, J. W.: Solar occultation satellite data and derived meteorological products: sampling issues and comparisons with Aura Microwave Limb Sounder, *J. Geophys. Res.*, 112, D24S50, doi:10.1029/2007JD008709, 2007. 31370

Manney, G. L., Santee, M. L., Rex, M., Livesey, N. J., Pitts, M. C., Veeckind, P., Nash, E. R., Wohltmann, I., Lehmann, R., Froidevaux, L., Poole, L. R., Schoeberl, M. R., Haffner, D. P., Davies, J., Dorokhov, V., Gernandt, H., Johnson, B., Kivi, R., Kyrö, E., Larsen, N., Levelt, P. F., Makshtas, A., McElroy, C. T., Nakajima, H., Parrondo, M. C., Tarasick, D. W., von der Gathen, P., Walker, K. A., and Zinoviev, N. S.: Unprecedented Arctic ozone loss in 2011, *Nature*, 478, 469–475, 2011. 31363, 31368, 31369, 31375

Martineau, P. and Son, S.-W.: Quality of reanalysis data during stratospheric vortex weakening and intensification events, *Geophys. Res. Lett.*, 37, L22801, doi:10.1029/2010GL045237, 2010. 31384

Mitchell, D. M., Charlton-Perez, A. J., and Gray, L. J.: Characterizing the variability and extremes of the stratospheric polar vortices using 2D moment analysis, *J. Atmos. Sci.*, 68, 1194–1213, 2011. 31370

Pawson, S.: Representation of the Middle-to-Upper Stratosphere in MERRA, Global Modeling and Assimilation Office Annual Report and Research Highlights, Greenbelt, Maryland, National Aeronautics and Space Administration Global Modeling and Assimilation Office, p. 42, 2012. 31367

Pawson, S. and Naujokat, B.: The cold winters of the middle 1990s in the northern lower stratosphere, *J. Geophys. Res.*, 104, 14209–14222, 1999. 31375

Pommereau, J.-P., Goutail, F., Lefèvre, F., Pazmino, A., Adams, C., Dorokhov, V., Eriksen, P., Kivi, R., Stebel, K., Zhao, X., and van Roozendaal, M.: Why unprecedented ozone loss in the Arctic in 2011? Is it related to climate change?, *Atmos. Chem. Phys.*, 13, 5299–5308, doi:10.5194/acp-13-5299-2013, 2013. 31364, 31377

## Comparisons of polar processing diagnostics

Z. D. Lawrence et al.

Title Page

Abstract

Introduction

Conclusions

References

Tables

Figures



Back

Close

Full Screen / Esc

Printer-friendly Version

Interactive Discussion



- Rex, M., Von Der Gathen, P., Braathen, G., Harris, N., Reimer, E., Beck, A., Alfier, R., Krüger-Carstensen, R., Chipperfield, M., De Backer, H., Balis, D., O'Connor, F., Dier, H., Dorokhov, V., Fast, H., Gamma, A., Gil, M., Kyrö, E., Litynska, Z., Mikkelsen, I., Molyneux, M., Murphy, G., Reid, S., Rummukainen, M., and Zerefos, C.: Chemical ozone loss in the arctic winter 1994/95 as determined by the match technique, *J. Atmos. Chem.*, 32, 35–59, doi:10.1023/A:1006093826861, 1999. 31376
- Rex, M., Salawitch, R. J., Gathen, P., Harris, N. R., Chipperfield, M. P., and Naujokat, B.: Arctic ozone loss and climate change, *Geophys. Res. Lett.*, 31, L04116, doi:10.1029/2003GL018844, 2004. 31364, 31377
- Rex, M., Salawitch, R. J., Deckelmann, H., von der Gathen, P., Harris, N. R. P., Chipperfield, M. P., Naujokat, B., Reimer, E., Allaart, M., Andersen, S. B., Bevilacqua, R., Braathen, G. O., Claude, H., Davies, J., De Backer, H., Dier, H., Dorokhov, V., Fast, H., Gerding, M., Godin-Beekmann, S., Hoppel, K., Johnson, B., Kyrö, E., Litynska, Z., Moore, D., Nakane, H., Parrondo, M. C., Risley, A. D., Skrivankova, P., Stübi, R., Viatte, P., Yushkov, V., and Zerefos, C.: Arctic winter 2005: implications for stratospheric ozone loss and climate change, *Geophys. Res. Lett.*, 33, L23808, doi:10.1029/2006GL026731, 2006. 31364, 31377
- Rieder, H. and Polvani, L. M.: Are recent Arctic ozone losses caused by increasing greenhouse gases?, *Geophys. Res. Lett.*, 40, 4437–4441, 2013. 31364, 31365, 31377
- Rienecker, M. M., Suarez, M. J., Gelaro, R., Todling, R., Bacmeister, J., Liu, E., Bosilovich, M. G., Schubert, S. D., Takacs, L., Kim, G.-K., Bloom, S., Chen, J., Collins, D., Conaty, A., Da Silva, A., Gu, W., Joiner, J., Koster, R. D., Lucchesi, R., Molod, A., Owens, T., Pawson, S., Pegion, P., Redder, C. R., Reichle, R., Robertson, F. R., Ruddick, A. G., Sienkiewicz, M., and Woollen, J.: MERRA: NASA's modern-era retrospective analysis for research and applications, *J. Climate*, 24, 3624–3648, 2011. 31366, 31368
- Saha, S., Moorthi, S., Pan, H.-L., Wu, X., Wang, J., Nadiga, S., Tripp, P., Kistler, R., Woollen, J., Behringer, D., Liu, H., Stokes, D., Grumbine, R., Gayno, G., Wang, J., Hou, Y.-T., Chuang, H.-Y., Juang, H.-M. H., Sela, J., Iredell, M., Treadon, R., Kleist, D., Delst, P. V., Keyser, D., Derber, J., Ek, M., Meng, J., Wei, H., Yang, R., Lord, S., van den Dool, H., Kumar, A., Wang, W., Long, C., Chelliah, M., Xue, Y., Huang, B., Schemm, J.-K., Ebisuzaki, W., Lin, R., Xie, P., Chen, M., Zhou, S., Higgins, W., Zou, C.-Z., Liu, Q., Chen, Y., Han, Y., Cucurull, L., Reynolds, R. W., Rutledge, G., and Goldberg, M.: The NCEP Climate Forecast System Reanalysis, *B. Am. Meteorol. Soc.*, 91, 1015–1057, 2010. 31384

**Comparisons of polar processing diagnostics**

Z. D. Lawrence et al.

Title Page

Abstract

Introduction

Conclusions

References

Tables

Figures



Back

Close

Full Screen / Esc

Printer-friendly Version

Interactive Discussion



- Santee, M. L., Tabazadeh, A., Manney, G. L., Fromm, M. D., Jensen, E. J., Bevilacqua, R. M., and Waters, J. W.: A Lagrangian approach to studying Arctic polar stratospheric clouds using UARS MLS  $\text{HNO}_3$  and POAM II aerosol extinction measurements, *J. Geophys. Res.*, 107, ACH 4-1–ACH 4-13, doi:10.1029/2000JD000227, 2002. 31364
- 5 Schoeberl, M. R. and Dessler, A. E.: Dehydration of the stratosphere, *Atmos. Chem. Phys.*, 11, 8433–8446, doi:10.5194/acp-11-8433-2011, 2011. 31365
- Schoeberl, M. R., Lait, L. R., Newman, P. A., and Rosenfield, J. E.: The structure of the polar vortex, *J. Geophys. Res.*, 97, 7859–7882, 1992. 31363, 31369
- Seviour, W. J. M., Mitchell, D. M., and Gray, L. J.: A practical method to identify displaced and split stratospheric polar vortex events, *Geophys. Res. Lett.*, 40, 5268–5273, doi:10.1002/grl.50927, 2013. 31370
- 10 Simmons, A. J., Hortal, M., Kelly, G., McNally, A., Untch, A., and Uppala, S.: ECMWF analyses and forecasts of stratospheric winter polar vortex break-up: September 2002 in the Southern Hemisphere and related events, *J. Atmos. Sci.*, 62, 668–689, 2005. 31365
- 15 Simmons, A. J., Poli, P., Dee, D. P., Berrisford, P., Hersbach, H., Kobayashi, S., and Peubey, C.: Estimating low-frequency variability and trends in atmospheric temperature using ERA-Interim, *Q. J. Roy. Meteor. Soc.*, 140, 329–353, 2014. 31368, 31373
- Sinnhuber, B.-M., Stiller, G., Ruhnke, R., von Clarmann, T., Kellmann, S., and Aschmann, J.: Arctic winter 2010/2011 at the brink of an ozone hole, *Geophys. Res. Lett.*, 38, L24814, doi:10.1029/2011GL049784, 2011. 31364
- 20 Solomon, S.: Stratospheric ozone depletion: a review of concepts and history, *Rev. Geophys.*, 37, 275–316, 1999. 31363, 31369
- Tilmes, S., Müller, R., Engel, A., Rex, M., and Russel, J. M.: Chemical ozone loss in the Arctic and Antarctic stratosphere between 1992 and 2005, *Geophys. Res. Lett.*, 33, L20812, doi:10.1029/2006GL026925, 2006. 31364, 31377
- 25 Waugh, D. W. and Randel, W. J.: Climatology of Arctic and Antarctic polar vortices using elliptical diagnostics, *J. Atmos. Sci.*, 56, 1594–1613, 1999. 31373
- Wegner, T., Grooß, J.-U., von Hobe, M., Stroh, F., Sumińska-Ebersoldt, O., Volk, C. M., Hösen, E., Mitev, V., Shur, G., and Müller, R.: Heterogeneous chlorine activation on stratospheric aerosols and clouds in the Arctic polar vortex, *Atmos. Chem. Phys.*, 12, 11095–11106, doi:10.5194/acp-12-11095-2012, 2012. 31369
- 30 WMO: Scientific assessment of ozone depletion: 2006, *Global Ozone Res. and Monit. Proj. Rep. 50*, Geneva, Switzerland, 2007. 31363

WMO: Scientific assessment of ozone depletion: 2010, Global Ozone Res. and Monit. Proj. Rep. 52, Geneva, Switzerland, 2011. 31363

5 Wohltmann, I., Wegner, T., Müller, R., Lehmann, R., Rex, M., Manney, G. L., Santee, M. L., Bernath, P., Sumińska-Ebersoldt, O., Stroh, F., von Hobe, M., Volk, C. M., Hösen, E., Ravegnani, F., Ulanovsky, A., and Yushkov, V.: Uncertainties in modelling heterogeneous chemistry and Arctic ozone depletion in the winter 2009/2010, Atmos. Chem. Phys., 13, 3909–3929, doi:10.5194/acp-13-3909-2013, 2013. 31369

Comparisons of polar processing diagnostics

Z. D. Lawrence et al.

Title Page

Abstract

Introduction

Conclusions

References

Tables

Figures



Back

Close

Full Screen / Esc

Printer-friendly Version

Interactive Discussion



## Comparisons of polar processing diagnostics

Z. D. Lawrence et al.

**Table 1.** Names of abbreviated instruments and satellites assimilated in ERA-Interim and MERRA.

Acronym	Full Name	Type
AIRS	Atmospheric Infrared Sounder	Instrument
AMSR	Advanced Microwave Scanning Radiometer	Instrument
AMSU	Advanced Microwave Sounding Unit	Instrument
ATOVS	Advanced Tiros Operational Vertical Sounder	System*
CHAMP	Challenging Minisatellite Payload	Satellite
COSMIC	Constellation Observing System for Meteorology, Ionosphere, and Climate	Satellite
GOES	Geostationary Operational Environmental Satellite	Satellites
HIRS	High resolution Infrared Radiation Sounder	Instrument
MHS	Microwave Humidity Sounder	Instrument
MSU	Microwave Sounding Unit	Instrument
SSM/I	Special Sensor Microwave Imager/Sounder	Instrument
SSU	Stratospheric Sounding Unit	Instrument
TOVS	Tiros Operational Vertical Sounder	System*

\* System denotes a suite of similar instruments used by a series of satellites.

Title Page

Abstract

Introduction

Conclusions

References

Tables

Figures



Back

Close

Full Screen / Esc

Printer-friendly Version

Interactive Discussion



Comparisons of polar processing diagnostics

Z. D. Lawrence et al.

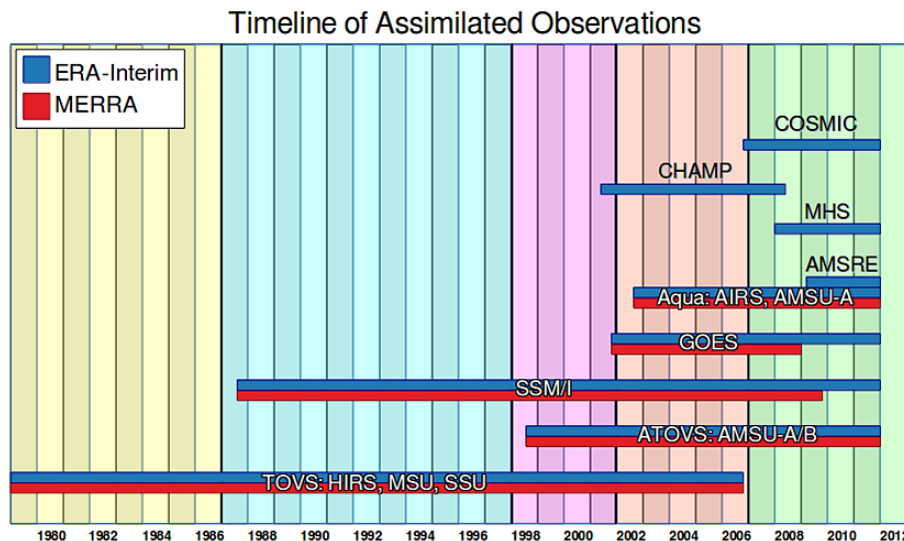


**Figure 1.** Timeline of satellite and GPSRO measurements assimilated in MERRA and ERA-Interim, organized by missions (when applicable) and instruments. Colored periods indicate regions of interest for intercomparisons, defined by significant changes in both data streams.

Title Page

Abstract

Introduction

Conclusions

References

Tables

Figures

◀

▶

◀

▶

Back

Close

Full Screen / Esc

Printer-friendly Version

Interactive Discussion



## Comparisons of polar processing diagnostics

Z. D. Lawrence et al.

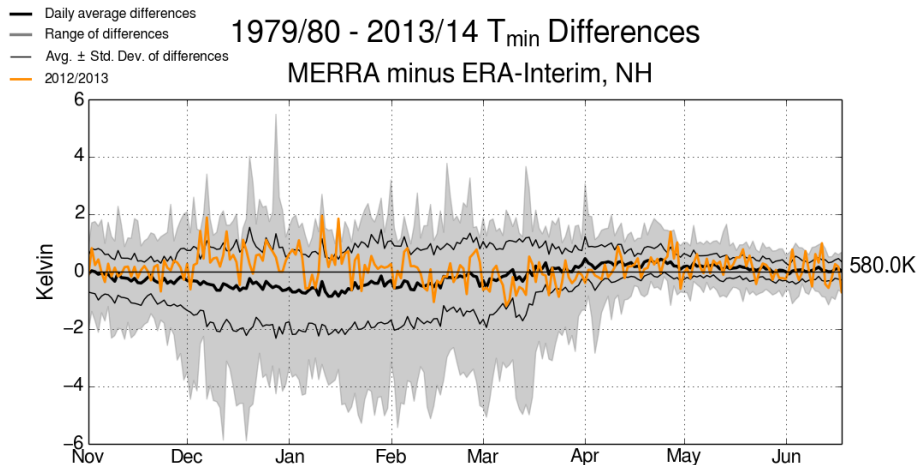


**Figure 2.** An example time series of the differences that are calculated for the daily diagnostics ( $T_{\min}$ ,  $A_{\text{PSC}}$ , etc.) that are in turn used to calculate monthly relative biases. This case shows the differences in  $T_{\min}$  between MERRA and ERA-I at 580 K for the 2012/2013 Arctic winter in orange, with the range of differences over all NH winters from 1979–2013 shown by the grey envelope. The thick black line represents the average daily differences over all years, while the thin black lines show one SD. Since the average daily differences vary over the seasons shown, we compute the monthly relative biases as the monthly means of the average daily differences.

[Title Page](#)
[Abstract](#)
[Introduction](#)
[Conclusions](#)
[References](#)
[Tables](#)
[Figures](#)

[Back](#)
[Close](#)
[Full Screen / Esc](#)
[Printer-friendly Version](#)
[Interactive Discussion](#)


## Comparisons of polar processing diagnostics

Z. D. Lawrence et al.

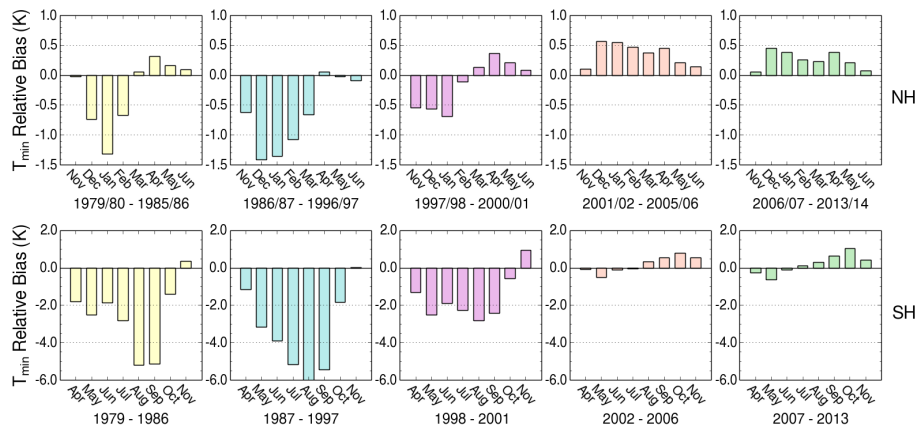


**Figure 3.** Monthly relative biases in  $T_{\min}$  between MERRA and ERA-Interim at 580 K potential temperature for Arctic (top) and Antarctic (bottom) winters. The colors used for the columns correspond to the colored regions of Fig. 1. The NH (SH) panels cover months from November through June (April through November).  $T_{\min}$  ( $y$  axis) scales are different for each hemisphere.

Title Page

Abstract

Introduction

Conclusions

References

Tables

Figures



Back

Close

Full Screen / Esc

Printer-friendly Version

Interactive Discussion



## Comparisons of polar processing diagnostics

Z. D. Lawrence et al.

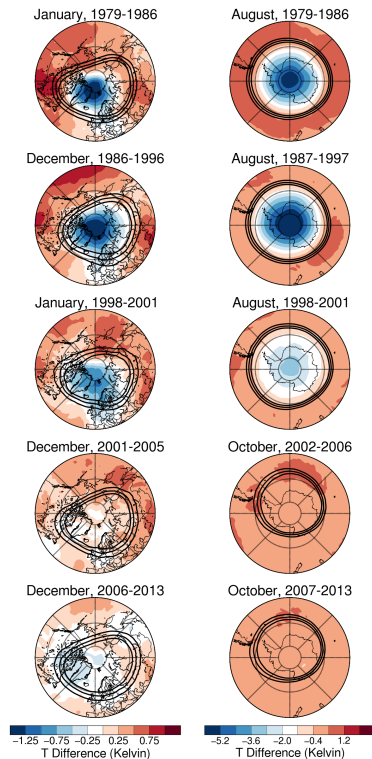


**Figure 4.** Maps of mean MERRA minus ERA-Interim 12:00 UT temperatures (averaged over the years listed) at 580 K potential temperature for the Arctic (left) and Antarctic (right) poleward of  $40^\circ$ . Contours of scaled potential vorticity from ERA-Interim in the vortex edge region are overlaid in black. The months shown correspond to the months with the largest  $T_{\min}$  relative biases, and the temperature scales are the same as shown in Fig. 3 (which differ for the Arctic and Antarctic).

[Title Page](#)[Abstract](#)[Introduction](#)[Conclusions](#)[References](#)[Tables](#)[Figures](#)[Back](#)[Close](#)[Full Screen / Esc](#)[Printer-friendly Version](#)[Interactive Discussion](#)

Comparisons of polar processing diagnostics

Z. D. Lawrence et al.

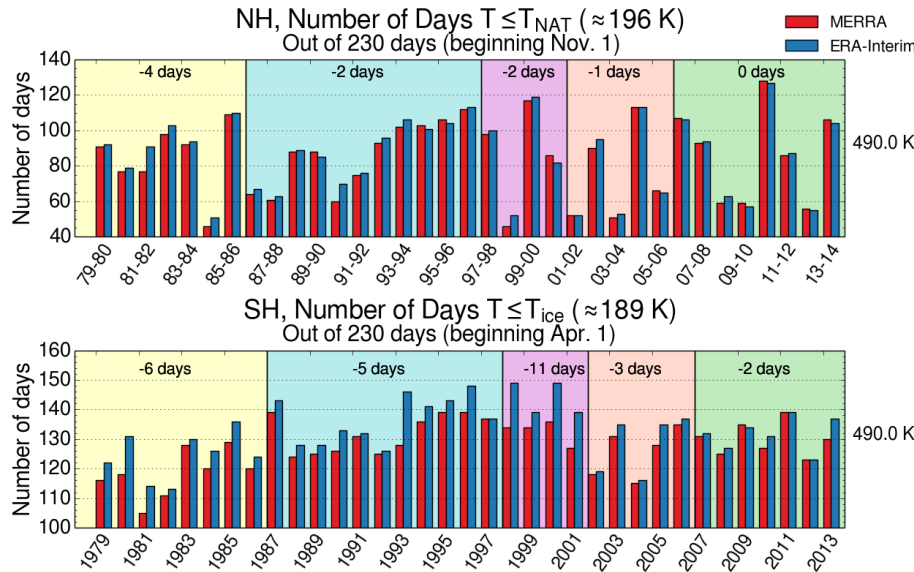


**Figure 5.** Number of days with Arctic (top) and Antarctic (bottom) winter minimum temperatures below NAT and ice PSC thresholds at 490 K. Note that the y axes do not start from zero, and have different ranges for each hemisphere. The black numbers at the top of each colored region indicate the average differences (MERRA minus ERA-I) for the time-period, rounded to the nearest day.

Title Page	
Abstract	Introduction
Conclusions	References
Tables	Figures
◀	▶
◀	▶
Back	Close
Full Screen / Esc	
Printer-friendly Version	
Interactive Discussion	



## Comparisons of polar processing diagnostics

Z. D. Lawrence et al.

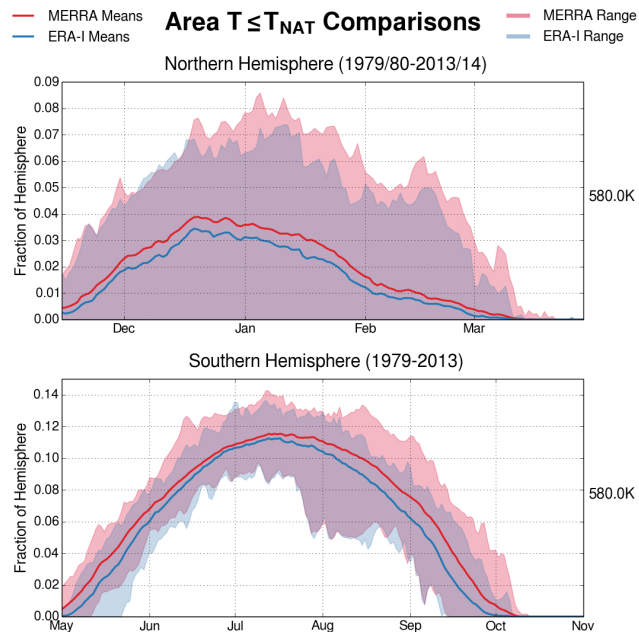


**Figure 6.** Mean values for  $A_{\text{NAT}}$  (thick red/blue lines) for Arctic and Antarctic winters at 580 K potential temperature. The blue (red) envelope shows the range of ERA-I (MERRA) values, with purple indicating where the ranges of the two reanalyses overlap.

## Comparisons of polar processing diagnostics

Z. D. Lawrence et al.

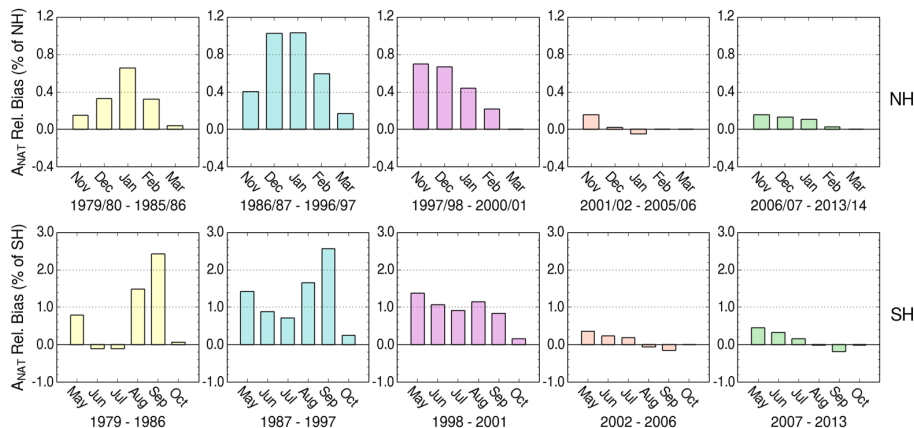


**Figure 7.** Monthly relative biases in  $A_{\text{NAT}}$  (% of hemisphere) between MERRA and ERA-Interim at 580 K potential temperature for Arctic (top) and Antarctic (bottom) winters. Time periods are as in Fig. 3. The NH (SH) panels cover months from November through March (May through October).  $A_{\text{NAT}}$  (y axis) scales are different for each hemisphere.

Title Page

Abstract

Introduction

Conclusions

References

Tables

Figures



Back

Close

Full Screen / Esc

Printer-friendly Version

Interactive Discussion



Comparisons of polar processing diagnostics

Z. D. Lawrence et al.

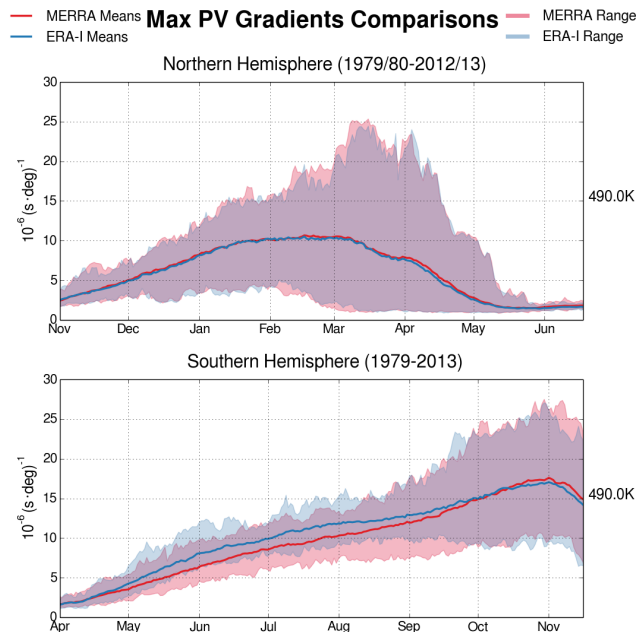


**Figure 8.** Mean values for maximum PV gradients (thick red/blue lines) for Arctic and Antarctic winters at 490 K potential temperature. The blue (red) envelope shows the range of ERA-I (MERRA) values, with purple indicating where the ranges of the two reanalyses overlap.

Title Page

Abstract Introduction

Conclusions References

Tables Figures

◀ ▶

◀ ▶

Back Close

Full Screen / Esc

Printer-friendly Version

Interactive Discussion



## Comparisons of polar processing diagnostics

Z. D. Lawrence et al.

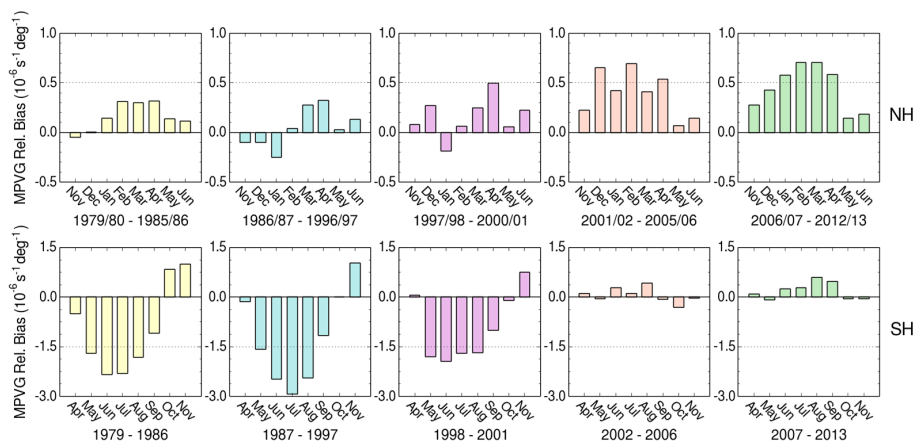


**Figure 9.** Monthly relative biases in maximum potential vorticity gradients between MERRA and ERA-Interim at 490 K potential temperature for Arctic (top) and Antarctic (bottom) winters. Time periods are as in Fig. 3. The NH (SH) panels cover months from November through June (April through November). MPVG ( $y$  axis) scales are different for each hemisphere.

Title Page

Abstract

Introduction

Conclusions

References

Tables

Figures



Back

Close

Full Screen / Esc

Printer-friendly Version

Interactive Discussion





## Comparisons of polar processing diagnostics

Z. D. Lawrence et al.

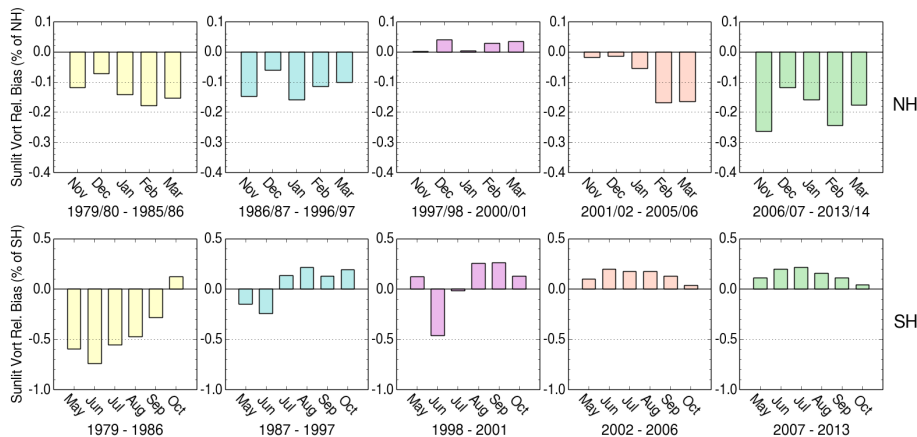


**Figure 11.** Monthly relative biases in sunlit vortex area between MERRA and ERA-Interim at 490 K potential temperature for Arctic (top) and Antarctic (bottom) winters. Time periods are as in Fig. 3. The NH (SH) panels cover months from November through March (May through October). Sunlit area ( $y$  axis) scales are different for each hemisphere.

Title Page

Abstract

Introduction

Conclusions

References

Tables

Figures



Back

Close

Full Screen / Esc

Printer-friendly Version

Interactive Discussion



Comparisons of polar processing diagnostics

Z. D. Lawrence et al.

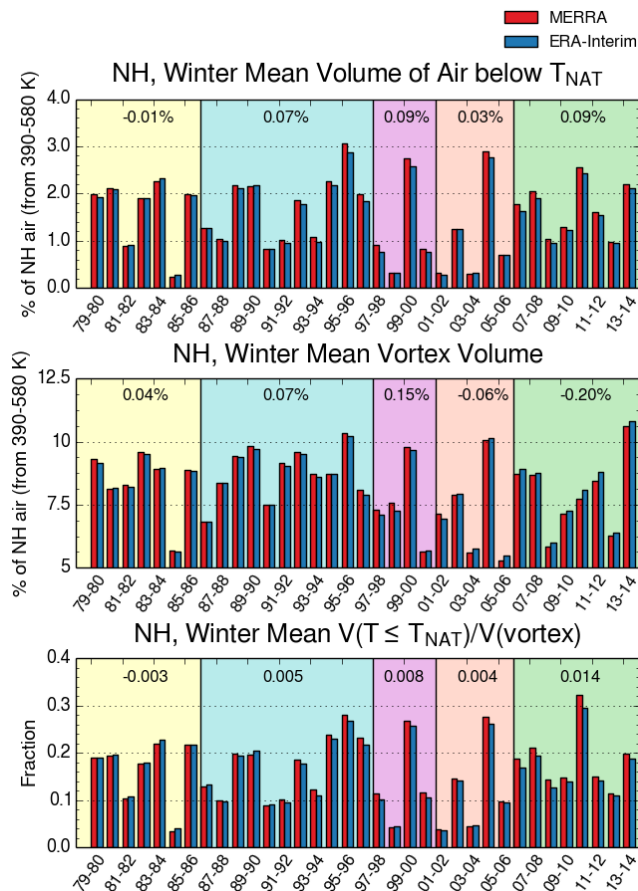


**Figure 12.** Arctic winter mean  $V_{PSC}$  (top),  $V_{vort}$  (center), and  $V_{PSC}$  expressed as a fraction of vortex volume (bottom). Note that the y axis for winter mean  $V_{vort}$  does not start from zero. The black numbers at the top of each colored region indicate the average differences (MERRA minus ERA-I) for the time-period.

Title Page

Abstract Introduction

Conclusions References

Tables Figures

◀ ▶

◀ ▶

Back Close

Full Screen / Esc

Printer-friendly Version

Interactive Discussion





Comparisons of polar processing diagnostics

Z. D. Lawrence et al.

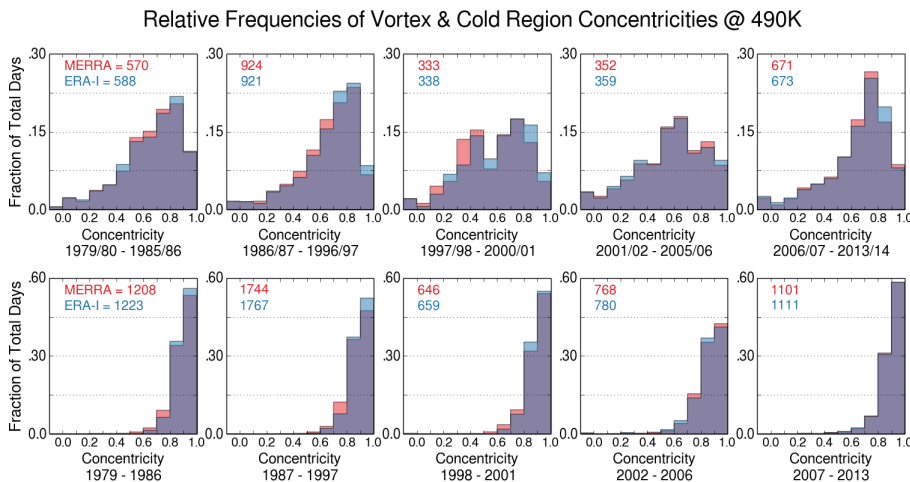


**Figure 14.** Concentricity of the polar vortex and regions with  $T \leq T_{\text{NAT}}$  expressed as relative frequencies of the total number of days with a valid concentricity value (red and blue numbers) from the time periods of Fig. 1 for Arctic (top) and Antarctic (bottom) winters.

Title Page

Abstract Introduction

Conclusions References

Tables Figures

◀ ▶

◀ ▶

Back Close

Full Screen / Esc

Printer-friendly Version

Interactive Discussion



## Comparisons of polar processing diagnostics

Z. D. Lawrence et al.

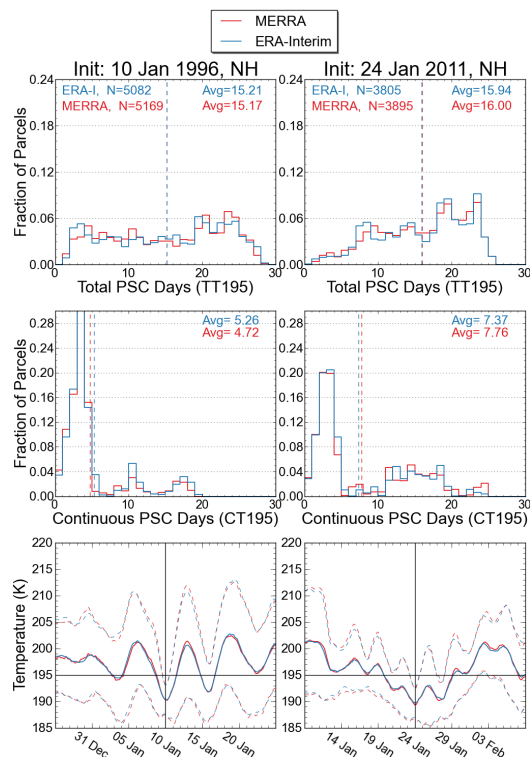


**Figure 15.** Temperature histories along air parcel trajectories at 490 K (~56 hPa). Both of the columns are from Arctic winters. The first and second rows are histograms of parcels that spent total and continuous time in temperatures below 195 K (see text). The dashed vertical lines show the averages of TT195 and CT195 for each of the reanalyses. The last row is the mean temperature of the parcels initialized in the cold regions for the full 30 day (15 day forward/backward) trajectory runs; the black vertical line indicates the initialization date, while the black horizontal line marks 195 K. The dashed red and blue curves show one SD range.

Comparisons of polar processing diagnostics

Z. D. Lawrence et al.

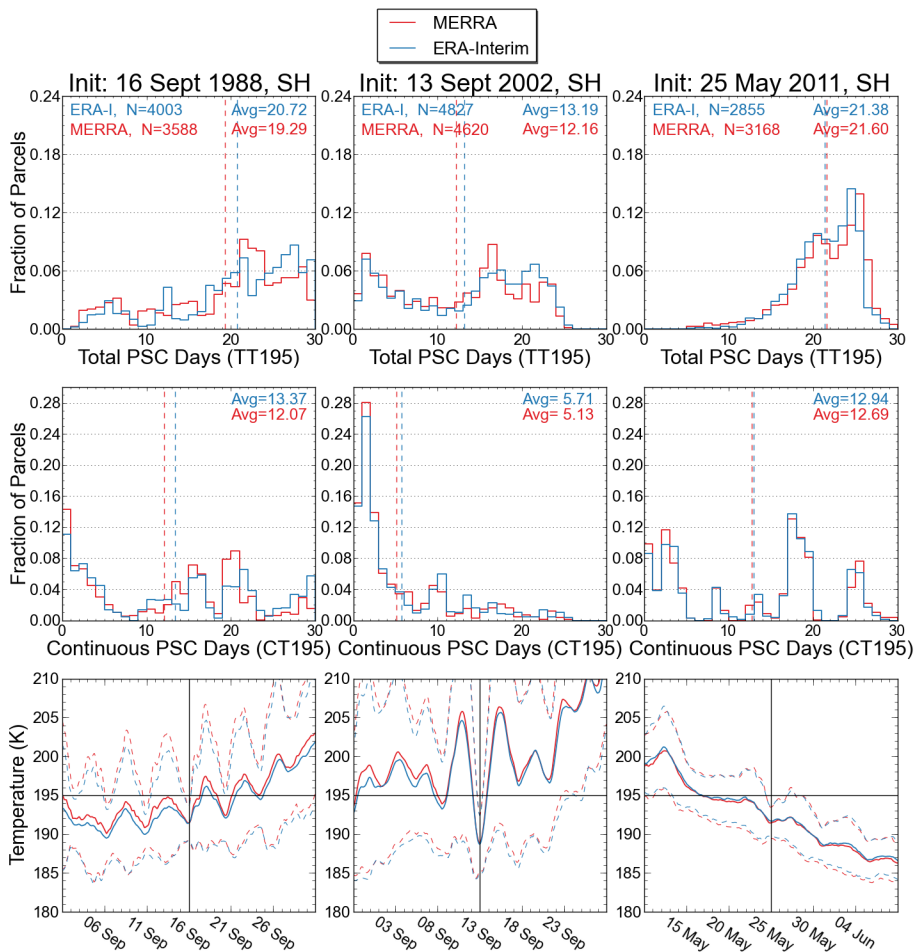


Figure 16. As in Fig. 15, but for Antarctic winters.

Title Page

Abstract Introduction

Conclusions References

Tables Figures

◀ ▶

◀ ▶

Back Close

Full Screen / Esc

Printer-friendly Version

Interactive Discussion

